

Design of a waveguide bandpass filter with inductive irises for a satellite application

*Amina Aghanim**, Rafik Lasri, Otman Oulhaj, and Hamid Chekenbah

Laboratory of science and advanced technologies, Abdelmalek Essaadi University, Tetouan, Morocco

Abstract. This paper presents a synthesis, design, and simulation of a bandpass rectangular waveguide filter with symmetrical transverse discontinuities operating in the X-band (WR90) with a central frequency of 11GHz, a fractional bandwidth of 3.1%, an undulation ripple of 0.014 dB inside the bandwidth, and a return loss level around 15 dB. The simulation is effectuated under the HFSS environment, where the results of the S-parameters in dB and degree were verified using a CST environment. The obtained results had proven the validity of the conception of our structure since it has shown a symmetrical aspect around the central frequency in both 3D simulators after optimizing the overall dimensions of the irises, also our study has proved that irises are a reliable way to design bandpass filters especially, where their dimensions mainly affect the filter response in terms of the return loss quantity, the insertion loss, and the filter's bandwidth.

Keywords: Filter, Bandpass, Discontinuity, Iris, Synthesis, and Waveguide.

1 Introduction

The growing interest in microwave applications and the overload utilization of the frequency bands had led to the saturating of the frequency spectrum [1]. This range was divided into a certain number of frequency bands, where each band was represented by a letter and dedicated to some specific applications. For example, several applications are operating in the L-Band (1-2GHz), such as GSM, CDMA, GPS, marine satellite, and military telemetry. While commercial applications using Bluetooth, or Wi-Fi are performing in the S-Band (2-4GHz). More the X-band (8-12GHz) is generally commercialized in military and industrial applications, especially with microwave waveguides [1-3]. In addition, satellite TV applications, VSAT, Radar, and astronomy applications are offered in the Ku and K-Band operating respectively in (12-18GHz) and (18-27GHz) ranges. As a result, establishing some filtering devices has become a major concern, since the frequency spectrum has become a limited source. Filters are devices having the ability to carry the energy thru some specific bands: passbands while rejecting and attenuating other frequencies in one or more stopbands.

Due to the growing interest in filtering devices, many types were developed and several classifications were adopted. An important classification has been done based on the chosen technology. The choice is generally effectuated based on the concrete requirements of the system in which the filter will be embedded. In the literature, three famous technologies are used while configuration: Planar technology, waveguide technology, and the substrate integrated waveguide (Substrate Integrated Waveguide, SIW) [4-5].

The filters designed based on waveguide technology are characterized by a high unload factor Q [6, 23], a low amount of losses, a huge power handling capacity, and a narrow bandwidth [7]. This technology rests on using

structures such as waveguides in either a rectangular or circular shape, metallic cavities, or dielectric resonators [8], more theoretical details about the fundamentals of waveguide resonators are elaborated in [23]. Unlike waveguide technology, filters made up using planar technology are typically designed by using some resonator on the top of a substrate. Concerning the unload factor, it should be noted that planar technology filters such as micro-strip filters have high insertion loss, a low unload factor, and selectivity, yet this technology has a lot of advantages like the miniaturization of the size of the device, the low cost, also its simple integration [7,9]. The SIW rests on realizing a dielectric rectangular waveguide in a planar substrate [10]. This technology takes advantage of both previous technologies by developing an outstanding unloaded quality factor, low cost, high power handling, and low loss [4,11].

This paper presents an overview of filter theory, the conception, and simulation of a 4th order waveguide bandpass filter operating in 11 GHz with inductive irises discontinuities. The simulation is effectuated under an HFSS environment. The remainder of this paper is arranged as follows: a methodological overview of the filter theory was elaborated in section two. Section three was committed to the conception phase of the bandpass filter. Then, the results are presented and discussed in section four where optimization of the irises dimensions was effectuated. The last section of this paper was dedicated to concluding and summarizing the overall obtained results.

2 Filter Theory

2.1 Filters characteristics

Considering microwave filters as complex systems, they could be characterized by many parameters such as

aghanimamina21@gmail.com

the filter order or degree, which could be defined as the number of components in the low pass prototype[6]. Also, the selectivity and the attenuation, which are essential filtering properties[12]. Selectivity describes the amount of change of the transmitted energy with respect to frequency. As well as the bandwidth that determines the range of frequency that the filter allows to transmit[6].

Many other parameters represent a reliable way to ensure the characterization of microwave filters and to describe the filter efficiency such as the return loss, the insertion loss, and the quality factor. Generally, the return loss[13] describes the effectiveness of power reflected by the load, while the insertion loss quantifies the energy received by the load [14]. These two parameters are expressed in terms of dB. In the microwave domain, the circuits are studied based on the S-parameters since the operating frequency range is high[15,16], their conception is quite simple and analytically appropriate. After all, a microwave filter is a two-port network, accordingly, it could be described in terms of the $S_{i,j}$ coefficients where i is the output port and j refers to the input port. S_{11} ($i=1, j=1$) Relates to the return loss in dB while S_{21} refers to the insertion loss quantity in dB.

2.2 Filters discontinuities

A discontinuity is an adjustment or a refitting inside the structure of the waveguide. The modification could be effectuated in terms of the direction of propagation, a change of the geometry, or the physical parameters. This, affects the translational symmetry of the waveguide structure and leads to energy reflections, and thus to the appearance of an impedance at the discontinuity [17,18].

It is worthy of note that irises are the most commonly used discontinuity, where they can produce an inductive or a capacitive effect based on their positioning. Therefore, they can take symmetrical or asymmetrical geometry.

Our study will shed light on the symmetrical inductive irises, the most familiar type of reactive discontinuities used in rectangular waveguides. The irises are placed in a parallel plane to the transverse face of the waveguide [19]. The relation between the normalized susceptance B and the distance between the irises are described in (1), (2), and (3).

$$B = \frac{2\pi}{\beta a} \cot^2 \left(\frac{\pi d}{2a} \right) \left[1 + \frac{a\gamma_3 - 3a}{4\pi} \sin^2 \left(\frac{\pi d}{a} \right) \right] \quad (1)$$

$$\beta = \sqrt{\omega^2 \epsilon \mu - \left(\frac{\pi}{a} \right)^2} \quad (2)$$

$$\gamma_3 = \sqrt{\left(\frac{3\pi}{a} \right)^2 - \omega^2 \epsilon \mu} \quad (3)$$

2.3 Synthesis of a waveguide bandpass filter with inductive irises process

In order to design a bandpass filter with irises in a waveguide technology, the method to follow consists generally of five steps[20]:

1. Design of a low pass filter prototype with localized elements.
2. Transformation of the low pass prototype to a bandpass filter.
3. Conversion of bandpass to impedance inverters K .
4. Calculation of the susceptance B and the electrical lengths Φ .

Calculation of the distances d using the previously calculated susceptance while the length of each iris is calculated using the flowing form: $l = \frac{a-d}{2}$.

The synthesis of the bandpass filter in waveguide technology is established based on a transformation in terms of wavelength instead of frequency, which is described with (4). The response then takes into account the central and cut-off wavelengths, which corresponds, to the central and the two cut-off frequencies of the waveguide. Therefore, the LC resonators were replaced with half-wavelength cavities and the irises by impedance inverters placed between each cavity. The coupling irises are simulated by $K_{i,i+1}$, these discontinuities present a purely inductive impedance characterized by the equations (5):(7) [20].

$$\Omega = \frac{1}{\Delta} \left(\frac{\lambda_{g0}}{\lambda_g} - \frac{\lambda_g}{\lambda_{g0}} \right) \quad (4)$$

$$\frac{K_{01}}{Z_0} = \sqrt{\frac{\pi \Delta}{2g_0 g_1}} \quad (5)$$

$$\frac{K_{j,j+1}}{Z_0} \Big|_{j=1, \dots, N-1} = \frac{\pi \Delta}{2\sqrt{g_j g_{j+1}}} \quad (6)$$

$$\frac{K_{N,N+1}}{Z_0} = \sqrt{\frac{\pi \Delta}{2g_N g_{N+1}}} \quad (7)$$

To establish the cavities length (8), (9), and (10) are involved:

$$\hat{B} = \frac{1 - \left(\frac{K}{Z_0} \right)^2}{\left(\frac{K}{Z_0} \right)} \quad (8)$$

$$\Phi = -\tan^{-1} \left(\frac{2}{\hat{B}} \right) \quad (9)$$

$$l_i = \frac{\lambda_{g0}}{2\pi} \left(\pi + \frac{\Phi_i}{2} + \frac{\Phi_{i+1}}{2} \right) \quad (10)$$

3 Conception of a waveguide Bandpass filter

To deepen the theory presented in the previous section, we have chosen a 4th bandpass filter with inductive irises designed in waveguide technology. This filter operates in the X-band (8-12 GHz), with a resonance frequency of 11 GHz and a relative bandwidth of 3.1%. The filter response is Chebyshev, with 20 dB reflection loss, the tolerated undulation ripples are of 0.014 dB inside the bandwidth and the input/output impedances are 50 Ω . Based on the Chebyshev equations, the numerical values of the normalized g_i parameters are illustrated in Table 1.

Table 1. Low Pass prototype Elements

g_0	g_1	g_2	g_3	g_4	g_5
1	0.931	1.292	1.577	0.762	1.221

The transformation of the low pass prototype in terms of wavelengths is presented in Table 2. Where λ_{g0} is the wavelength corresponding to the resonance frequency, where λ_{g1} and λ_{g2} are the wavelengths of the two cut-off frequencies.

Table 2. Numerical values of the wavelengths in mm

λ_{g0}	λ_{g1}	λ_{g2}
0.034	0.034	0.033

The relative bandwidth is calculated using (11) and gives 4.16%:

$$\Delta = \frac{\lambda_{g1} - \lambda_{g2}}{\lambda_{g0}} \quad (11)$$

Table 3 illustrates the characteristic impedances of the inverters, obtained (5), (6), and (7).

Table 3. Inverter impedances numerical values

K_{01}	K_{12}	K_{23}	K_{34}	K_{45}
0.265	0.059	0.045	0.059	0.265

After calculating the inverter's numerical values, the next step is to determine the numerical values of the susceptance $B_{i,j}$ and the phase shift $\Phi_{i,j}$ in radian, based on (8) and (9). Table 4 summarizes the results.

Table 4. Irises susceptance B_{ij} and phase shifts Φ_{ij}

$B_{01}=3.507$	$B_{12}=16.698$	$B_{23}=21.763$	$B_{34}=16.698$	$B_{45}=3.507$
$\Phi_{01}=-0.518$	$\Phi_{12}=-0.119$	$\Phi_{23}=-0.091$	$\Phi_{34}=-0.119$	$\Phi_{45}=-0.518$

Typically, these phase shifts are subtracted from the phase shifts of the half-wave resonant cavities, which allows determining the lengths of the cavities, and the numerical values of the distances between the symmetrical inductive irises are depicted in Table 5.

Table 5. Electrical lengths of the cavities

Φ_l (rad)	$\Phi_1 = 2.504$	$\Phi_2 = 2.930$	$\Phi_3 = 2.930$	$\Phi_4 = 2.504$	
l_i (mm)	$l_1 = 14.705$	$l_2 = 15.859$	$l_3 = 15.859$	$l_4 = 14.705$	
d_i	$d_1 = 9.40$	$d_2 = 5.22$	$d_3 = 4.72$	$d_4 = 5.22$	$d_5 = 9.40$

The different numerical values of the distances between the symmetrical inductive irises are depicted in Table 6 according to the filter specifications, which are obtained from the Matlab script.

4 Results and discussion

The structure under consideration is a metallic rectangular waveguide, with symmetrical inductive transverse discontinuities. Accordingly, five irises separate between the four cavities. The standard WR-90 waveguide, with its operating frequency range from 8 GHz to 12 GHz, where the chosen central frequency is 11GHz. The cut-off frequency for the lowest mode is 6.56 GHz according to the transverse dimensions of waveguide $a=22.86\text{mm}$ and $b=10.16\text{mm}$. The inductive irises appear as an opening at the end of the cavities or as a narrowing of the guide after each half wavelength. Assuming that the thickness of all irises is the same in the design process $t = 2\text{mm}$. Also, our design is characterized by five discontinuities, the topology of the filter is obtained in Fig.1.

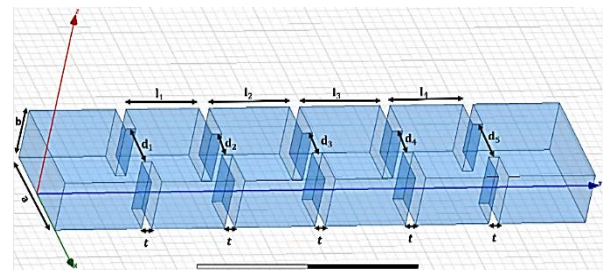


Fig. 1. Topology of the waveguide filter with irises.

Using the results of Table 5, the simulation was accomplished under the HFSS environment. However, the filter does not meet the specifications set for our filter according to the variation of the S-parameters shown in Fig.2.

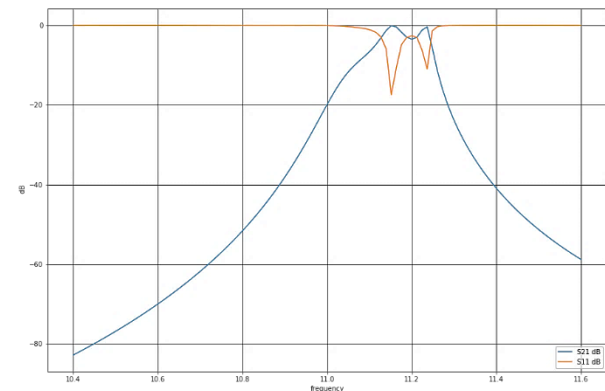


Fig. 2. The simulated S-parameters in HFSS.

The depicted results are not responding to the fixed specifications. Therefore, a call for optimizing the dimensions of the irises was necessary to improve the S-parameters of our filter. Table 6 summarizes the optimized dimensions of the inductive irises.

Table 6. Optimized dimensions of the irises in mm

$d_1 = d_5 = 10.27$	$d_2 = 6.65$	$d_3 = 6.18$	$d_4 = 6.65$
---------------------	--------------	--------------	--------------

$l_1 = 14.29$	$l_2 = 15.73$	$l_3 = 15.73$	$l_4 = 14.29$
---------------	---------------	---------------	---------------

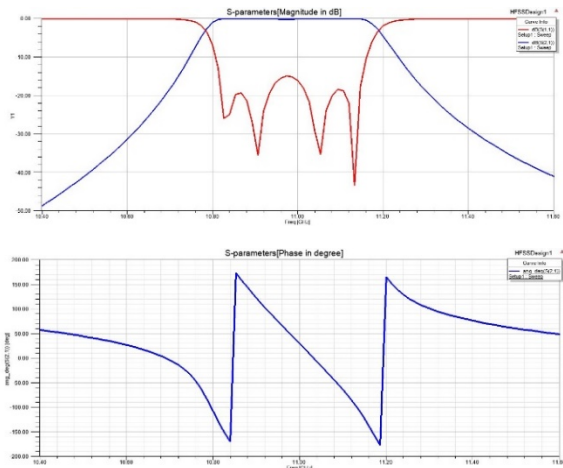


Fig. 3. The simulated S-parameters in dB and S_{21} in degree under HFSS

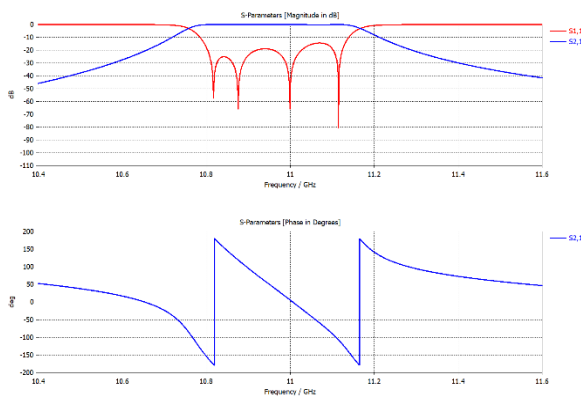


Fig. 4. The simulated S-parameters in dB and S_{21} in degree under CST

As it is shown in both Fig.3 and Fig.4, the variation of the S-parameters could be considered highly close to the target in both simulators, either CST or HFSS. Besides, the insertion loss quantity shows a symmetrical aspect around the resonance frequency 11GHz, which could be considered as a good result after optimizing the dimensions of the irises.

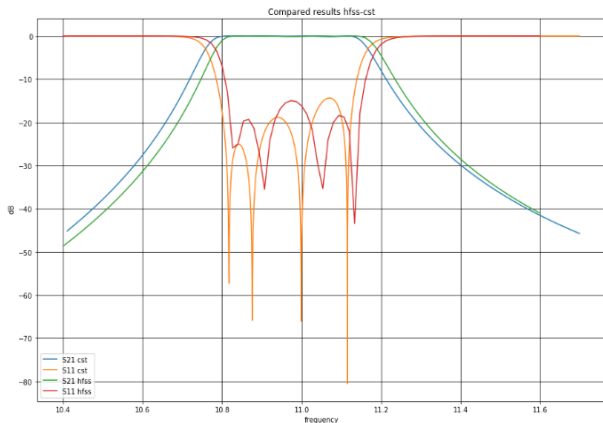


Fig. 5. The simulated S-parameters in HFSS and CST.

In Fig.5 the simulated S-parameters responses are compared and analysed in two previously mentioned 3D-Simulators HFSS and CST to validate the conception results. As shown, the simulated results present an appearance close to the fixed specifications of our filter after the optimization process. Where the reflection level is around 16 dB in the entire passband, also the lower and upper cut-off frequencies are around 10.8 GHz and 11.2 GHz while the quantity of the insertion loss remains 0 dB in the whole

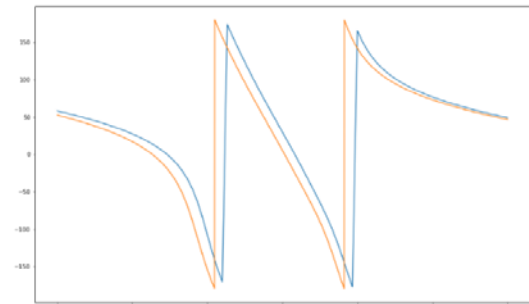


Fig. 6. The simulated results of the phase of S_{21} in HFSS and CST

We can see from the graph of Fig.6 that the obtained results of S_{21} in degree had met the required specifications. A symmetrical aspect at the resonance frequency was present, where the phase passes through $\pm 180^\circ$ and 0° crossing at the center frequency.

The performance of the concerned filter is compared with two other pre-existing Filters, and analysis are presented in Table.7

Table.7. Optimized dimensions of the irises in mm

Reference	[21]	[22]	[2]	Proposed design
Filter dimensions (mm ²)	64x32	8.64x4.32	22.86x10.16	22.86x10.16
Type of the irises	Rectangular	Circular	Rectangular	Rectangular
Frequency (GHz)	4.55	28	10	11
Number of irises	3	6	6	5
Thickness of irises(mm)	1	varying	3	2
Return loss (dB)	17	15	18	15

5 Conclusion

In this paper, the conception of a bandpass filter in waveguide technology and inductive irises separating the resonant cavities has been elaborated. The filter is operating in the X-band (WR90) with a resonance

frequency of 11 GHz. The obtained results had confirmed that the conception met the previously fixed specifications, especially after optimizing the dimensions of each iris, which was shown based on the symmetrical aspect of S_{21} in degree around 11 GHz. Later on, short-term prospects had been fixed, such as realizing and testing the simulated structure in order to compare the proposed simulated results and the measured ones, in order to validate the design process.

References

1. S. Wu, W. Cao, M. Wu, and C. Liu, International Journal of Electronics and Communication Engineering **12**, 7 (2018)
2. M. AbuHussain and U. C. Hasar, Electronics **9**, 101 (2020)
3. V. Boria and B. Gimeno, IEEE Microwave **8**, 60 (2007)
4. M. Le Coq, E. Rius, J.-F. Favennec, C. Quendo, B. Potelon, L. Estagerie, P. Moroni, B. Bonnet, and A. El Mostrah, IEEE Trans. Compon., Packag. Manufact. Technol. **5**, 620 (2015)
5. V. Sekar, M. Armendariz, and K. Entesari, IEEE Trans. Microwave Theory Techn. **59**, 866 (2011)
6. R. J. Cameron, C. M. Kudsia, and R. R. Mansour, *Microwave Filters for Communication Systems: Fundamentals, Design and Applications*, 2nd ed (Wiley, Hoboken, 2018)
7. I. C. Hunter, L. Billonet, B. Jarry, and P. Guillon, IEEE Trans. Microwave Theory Techn. **50**, 794 (2002)
8. R. Levy, R. V. Snyder, and G. Matthaei, IEEE Trans. Microwave Theory Techn. **50**, 783 (2002)
9. A. M. Abbosh, IEEE Trans. Microwave Theory Techn. **55**, 2262 (2007)
10. I. Aram, K. Garb, and R. Kastner, in *2014 IEEE 28th Convention of Electrical & Electronics Engineers in Israel (IEEEI)* (IEEE, Eilat, Israel, 2014)
11. Q.-L. Zhang, W.-Y. Yin, S. He, and L.-S. Wu, PIER **111**, 419 (2011)
12. A. E. Atia and A. E. Williams, IEEE Trans. Microwave Theory Techn. **20**, 258 (1972)
13. T. S. Bird, IEEE Antennas Propag. Mag. **5**(2009)
14. R. W. Beatty, Proc. IEEE **52**, 663 (1964)
15. S. Wang, F. C. Lee, and W. G. Odendaal, IEEE Trans. Power Electron. **20**, 502 (2005)
16. J. CARLIN, IRE Trans. Circuit Theory **10** (1956)
17. D. Sun and J. Xu, IEEE Microw. Wireless Compon. Lett. **26**, 475 (2016)
18. Y. Zhai, Q. Wang, Z. Wang, and X. xiao Gao, in *2008 Global Symposium on Millimeter Waves* (IEEE, Nanjing, China, 2008), pp. 348–350
19. M. S. Anwar and H. R. Dhanyal, in *2018 15th International Bhurban Conference on Applied Sciences and Technology (IBCAST)* (IEEE, Islamabad, 2018), pp. 866–869
20. D. M. Pozar, Microwave engineering, 4th ed (Wiley, 2011)
21. S. Chooadee and S. Akatimagool, EEE **2**, 152 (2012)
22. Y. P. Lim, C. Sovuthy, and P. W. Wong, IJACEN, **6** (2018)